journal

J. Am. Ceram. Soc., 73 [1] 54-60 (1990)

# Sintering with Rigid Inclusions: Pair Interactions

S. Sundaresan† and Ilhan A. Aksay*

Department of Materials Science and Engineering, and Advanced Materials Technology Program, Washington Technology Center, University of Washington, Seattle, Washington 98195

**The interaction between two spherical, rigid inclusions in an infinite, linearly viscous, densifying medium has been studied. The stresses in the vicinity of the two spheres are highly anisotropic, with significantly enhanced rates of densification in the gap between these particles. A pairwise-additive approximation for the densification rate of the composite is presented and compared with the composite-sphere and self-consistent models described by Scherer. [Key words: sintering, modeling, inclusions, composites, stress.]**

## I. Introduction

THE effect of inclusions and heterogeneities on the sintering process has been a subject of many theoretical and experimental studies.[1-15] A reduction in the rate of densification caused by the presence of these inclusions is well documented in the literature. Furthermore, differential shrinkage characteristics of the matrix and the inclusions or heterogeneities may give rise to sintering damage, such as cracklike flaws, planar array of voids, or isolated pores.[3,8,9]

The development of stresses during the sintering process has been examined theoretically by several authors.[1-6,11] Some of these studies predicted that very large tensile stresses can evolve in the matrix containing the inclusions, but it has been pointed out by Scherer[1] and Bordia and Scherer[11] that these large stresses are due to inconsistent constitutive models (resulting in a negative Poisson's ratio) used in these studies. They argued that the magnitudes of the radial and hoop stresses around a rigid inclusion in a sintering matrix cannot exceed $2\Sigma$ and $\Sigma$, respectively, where $\Sigma$ is the so-called sintering pressure due to reduction in surface area. Their assertion is based on a composite-sphere model. In this model, the sintering matrix containing multiple heterogeneities is idealized through a single inclusion surrounded by a matrix whose size is chosen to obtain the same volume fraction of inclusion as in the real problem. Such a model does not account for the interactions between the inclusions in an entirely satisfactory manner. These interactions become more and more important as the number density of the inclusions increases. Although these interactions are many-body in nature, one may, at least as a start, treat them as pairwise-additive. In such an approximation, the fundamental problem is to understand the interactions between two inclusions in an infinite densifying matrix, the analysis of which is the objective of the present study. We shall restrict our attention to rigid, spherical inclusions of uniform size in an infinite densifying medium (henceforth simply referred to as the matrix).

The well-known case of a single inclusion in an infinite matrix[1,2,5] will be described briefly in Section II. It will be seen later that the results of the single-inclusion problem will serve as the far-field solution for the two-inclusions problem which will be described in Section III. The results of the two-inclusions problem will be presented in Section IV, where it will be shown that local stresses in excess of the upper bound of Scherer[1] and Bordia and Scherer[11] can arise when the interactions between two inclusions are taken into account. The densification rate of a matrix containing many rigid inclusions, obtained by treating the interactions between the inclusions as pairwise-additive, will be compared in Section V with the predictions of other models in the literature.

An expression for the effective interaction between two inclusions in a composite arising from the excluded-volume effect will be derived in Section VI. It will be shown that the matrix between inclusion pairs of large separations will be in a state of tension, whereas the matrix between pairs of smaller separation will be in compression, as suggested by Lange.[10] Finally, the findings of the present study will be summarized in Section VII.

## II. Single Inclusion in an Infinite Matrix

Consider a rigid spherical inclusion of radius $R_o$ surrounded by an infinite matrix. In the matrix

$$\nabla \cdot \boldsymbol{\sigma} = \mathbf{0} \tag{1}$$

where $\boldsymbol{\sigma}$ is the stress tensor. Following Scherer[1] and Bordia and Scherer,[11] we shall neglect the elastic response of the matrix and assume that the relationship between the stress and the rate of strain is linear. Then

$$\boldsymbol{\sigma} = 2G_m\left\{\frac{1}{2}[\nabla\mathbf{u} + (\nabla\mathbf{u})^T] - \frac{1}{3}(\nabla\cdot\mathbf{u})\boldsymbol{I}\right\} + K_m(\nabla\cdot\mathbf{u} - 3\dot{\varepsilon}_f)\boldsymbol{I} \tag{2}$$

where $G_m$ is the shear viscosity of the matrix, $K_m$ the bulk viscosity of the matrix, $\dot{\varepsilon}_f$ the linear densification rate of the unconstrained matrix, $\mathbf{u}$ the velocity, and $\boldsymbol{I}$ the identity tensor. The development of constitutive models for $G_m$, $K_m$, and $\dot{\varepsilon}_f$ from microscopic considerations of shear and densification is an important part of sintering theories, but is not the focus of the present analysis. Instead, we shall assume that these quantities are known (and uniform everywhere in the matrix) and focus on the role of the inclusions. One can define an apparent Poisson's ratio for the matrix, $\nu_m$, by

$$\frac{2G_m}{3K_m} = \frac{1 - 2\nu_m}{1 + \nu_m} \tag{3}$$

where, as pointed out by Scherer,[1] $0 \le \nu_m \le \frac{1}{2}$. In terms of a spherical coordinate system whose origin coincides with the center of the spherical inclusion, the boundary conditions for Eq. (1) become

$$\mathbf{u} = \mathbf{0} \quad (\text{at } r = R_o)$$
$$\sigma_{rr} = -p_\infty \quad (\text{as } r \to \infty) \tag{4}$$

where $\sigma_{rr}$ is the normal stress in the radial direction and $p_\infty$ is the external compressive stress imposed on the matrix. By spherical symmetry, $\mathbf{u} = u\mathbf{e}_r$ where $\mathbf{e}_r$ is the unit vector in the

Manuscript No. 198805. Received October 31, 1988; approved May 15, 1989.

Supported by the Air Force Office of Scientific Research (AFOSR) and the Defense Advanced Research Project Agency (DARPA) and monitored by AFOSR under Grant No. AFOSR-87-0114.

*Member, American Ceramic Society.

†Permanent address: Department of Chemical Engineering, Princeton University, Princeton, NJ 08544.

radial direction. It is straightforward to solve Eqs. (1) and (2) with the boundary conditions given by Eq. (4), and one obtains

$$u = \left(1 + \frac{p_\infty}{\Sigma}\right)\dot{\varepsilon}_f r\left(1 - \frac{R_o^3}{r^3}\right) \tag{5}$$

where $\Sigma$, the so-called sintering pressure, is equal to $-3K_m\dot{\varepsilon}_f$. It follows that on the surface of the inclusion

$$\sigma_{rr} = 3K_m\left[\frac{3(1-\nu_m)}{1+\nu_m}\left(1 + \frac{p_\infty}{\Sigma}\right) - 1\right]\dot{\varepsilon}_f \tag{6}$$

For later use, we observe the following: (a) for $r \gg R_o$, Eq. (5) reduces to

$$u = \left(1 + \frac{p_\infty}{\Sigma}\right)\dot{\varepsilon}_f r \equiv u_\infty(r) \tag{7}$$

and (b) a translation of the origin from the center of the spherical inclusion by a distance $C_o$ in any direction would imply from Eq. (5) that the velocity of the spherical inclusion toward this new origin, $U_{o1}$, is given by

$$U_{o1} = -\left(1 + \frac{p_\infty}{\Sigma}\right)\dot{\varepsilon}_f C_o(1 - R_o^3/C_o^3) \tag{8a}$$

With the reference inclusion at origin, let us imagine placing a second test sphere in the matrix such that the center-to-center separation is $2C_o$. If this test sphere simply responds to the streamlines in the matrix without perturbing it appreciably, then this sphere will move toward the origin at a velocity $U_{o2}$ given by

$$U_{o2} = -2\left(1 + \frac{p_\infty}{\Sigma}\right)\dot{\varepsilon}_f C_o(1 - R_o^3/8C_o^3) \tag{8b}$$

If the two spheres are strictly noninteracting, they would approach each other at a velocity $2U_{o1}$. The approach velocity described by Eq. (8*b*) is usually referred to as the far-field interaction. Note that $U_{o2} > 2U_{o1}$; thus the far-field interaction is attractive in the sintering problem. At close separations, Eq. (8*b*) is certainly incorrect, as the resistance to viscous deformation of the matrix in the region between the spheres will give rise to an effective repulsion and slow down the approach velocity. This near-field correction is analyzed in the next section.

## III. Two Spherical Inclusions in an Infinite Matrix

Consider two rigid spherical inclusions of radius $R_o$ located such that the center-to-center distance is equal to $2C_o$. We shall choose a Cartesian coordinate system such that the $z$ axis is the line of centers and the centers of the spheres are located at $(0,0,\pm C_o)$. It is easily seen that as densification occurs the two spheres will move toward each other. We shall denote the speed of each sphere toward the origin by $W_o$. If the densification proceeds with little interaction between the two spheres, then $W_o = U_{o1}$. In the limit of only far-field interaction, $W_o = U_{o2}/2$. In order to determine the stresses developed at various locations, we must now solve Eqs. (1) and (2) along with the following boundary conditions:

$$\sigma_{xx}, \sigma_{yy}, \sigma_{zz} \to -p_\infty \quad (\text{as } r \to \infty) \tag{9}$$

where

$$r = (x^2 + y^2 + z^2)^{1/2} \tag{10}$$

On the surface of the sphere located at $z = C_o$

$$\mathbf{u} = -W_o\mathbf{e}_z \tag{11}$$

while on the sphere located at $z = -C_o$

$$\mathbf{u} = W_o\mathbf{e}_z \tag{12}$$

One can readily anticipate that the velocities far away from the spheres would follow Eq. (7).

It is convenient to scale the stress tensor as

$$\boldsymbol{\sigma}^* = -\frac{\boldsymbol{\sigma}/\Sigma - \mathbf{I}}{p_\infty/\Sigma + 1} \tag{13}$$

so that

$$\sigma^*_{xx}, \sigma^*_{yy}, \sigma^*_{zz} \to 1 \quad (\text{as } r \to \infty) \tag{14}$$

It is easy to show from Eqs. (2) and (13) that the linear densification rate, $\dot{\varepsilon}$, at any point in the matrix is given by

$$3\dot{\varepsilon} = \nabla\cdot\mathbf{u} = \left(\frac{p_\infty}{\Sigma} + 1\right)\dot{\varepsilon}_f \operatorname{tr}[\boldsymbol{\sigma}^*] \tag{15}$$

Noting that as $r \to \infty$, $\operatorname{tr}[\boldsymbol{\sigma}^*] \to 3$, we can write that

$$\dot{\varepsilon} = \frac{1}{3}\dot{\varepsilon}_\infty \operatorname{tr}[\boldsymbol{\sigma}^*] \tag{16}$$

where

$$\dot{\varepsilon}_\infty = \left(\frac{p_\infty}{\Sigma} + 1\right)\dot{\varepsilon}_f \tag{17}$$

is the linear densification rate at points far away from the spherical inclusions.

The solution of this system of equations has already been reported by Shelley and Yu[16] and will not be repeated here. Briefly, the torsion-free rotational symmetry about the $z$ axis and the absence of any body force in the model equations permit the general solution to be written as the sum of two velocity fields $\mathbf{u}_1$ and $\mathbf{u}_2$

$$2G_m\mathbf{u}_1 = \nabla\Phi \tag{18}$$

$$2G_m\mathbf{u}_2 = \nabla(z\Psi) - 4(1-\nu_m)\Psi\mathbf{e}_z \tag{19}$$

and $\mathbf{u} = \mathbf{u}_1 + \mathbf{u}_2$. Here $\Phi(r,z)$ and $\Psi(r,z)$ (with $r$ being given by Eq. (10)) satisfy

$$\nabla^2\Phi = \nabla^2\Psi = 0 \tag{20}$$

The functions $\Phi$ and $\Psi$ must be so chosen to satisfy the boundary conditions. It has been found to be convenient to analyze the problem in a spherical bipolar coordinate system defined by

$$x = \frac{R_o \sinh\alpha_o \sin\beta\cos\gamma}{\cosh\alpha - \cos\beta}$$

$$y = \frac{R_o \sinh\alpha_o \sin\beta\sin\gamma}{\cosh\alpha - \cos\beta}$$

$$z = \frac{-R_o \sinh\alpha_o \sinh\alpha}{\cosh\alpha - \cos\beta} \tag{21}$$

where $-\infty < \alpha < \infty$, $0 \le \beta \le \pi$, $0 \le \gamma \le 2\pi$ and $\alpha_o$ is given by

$$C_o = R_o \cosh\alpha_o \tag{22}$$

In the spherical bipolar coordinate system,[16,17] the surfaces of the spherical inclusions located at $z = \pm C_o$ are described by $\alpha = \mp\alpha_o$. The region occupied by the matrix is $-\alpha_o \le \alpha \le \alpha_o$, $0 \le \beta \le \pi$, $0 \le \gamma \le 2\pi$. Figure 1 describes the geometry and the unit vectors on the spherical bipolar coordinate system. It is easily seen that the scaled normal stress acting in a direction perpendicular to the surface of the inclusion would be $\sigma^*_{\alpha\alpha}$, while $\sigma^*_{\beta\beta}$ and $\sigma^*_{\gamma\gamma}$ are the scaled hoop stresses. There can also be a scaled shear stress $\sigma^*_{\alpha\beta}$ on this surface. (From symmetry considerations, $\sigma^*_{\alpha\gamma} = \sigma^*_{\beta\gamma} = 0$.) The net force acting on the sphere at $\alpha = \alpha_o$ can be written as[16]

$$\mathbf{F}(W_o, C_o/R_o) = \mathbf{e}_z\{\int_A[\sigma_{\alpha\alpha}\cos(\alpha,z) + \sigma_{\alpha\beta}\cos(\beta,z)]\,dA\} \tag{23}$$

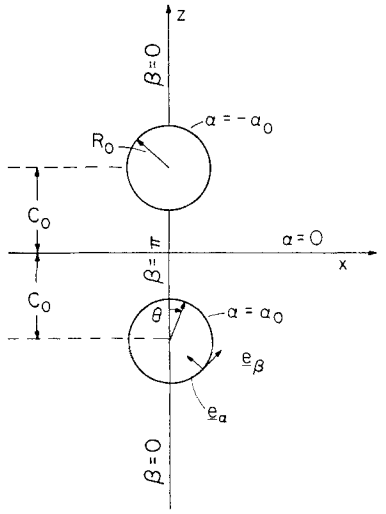


**Fig. 1.** Schematic representation of the two-sphere geometry and the unit vectors in the spherical bipolar coordinates. The $y$ axis in the Cartesian coordinate system and the $\gamma$ axis in the spherical bipolar coordinate system are perpendicular to the plane of the paper.

where

$$\cos(\alpha,z) = \frac{\cosh\alpha\cos\beta - 1}{\cosh\alpha - \cos\beta}$$

$$\cos(\beta,z) = \frac{\sinh\alpha\sin\beta}{\cosh\alpha - \cos\beta} \tag{24}$$

and the integration is performed over the surface of this sphere. After some algebraic manipulations it can be shown that

$$\mathbf{F}(W_o,C_o/R_o) = 2\pi R_o^2 \sinh^2\alpha_o\left(1 + \frac{p_\infty}{\Sigma}\right)\Sigma\mathbf{e}_z \times \left\{\int_0^\pi [\sigma^*_{\alpha\alpha}\cos(\alpha,z) + \sigma^*_{\alpha\beta}\cos(\beta,z)]_{\alpha=\alpha_o} \times \frac{\sin\beta\, d\beta}{(\cosh\alpha_o - \cos\beta)^2}\right\} \tag{25}$$

One can define a scalar, scaled interparticle force acting along the line of centers according to

$$f(W_o,C_o/R_o) = -|\mathbf{F}|/R_o^2\Sigma\left(1 + \frac{p_\infty}{\Sigma}\right) \tag{26}$$

so that a negative $f$ implies attractive interaction between the particles.

There are two cases of particular interest in the present problem. First, we would like to compute the force experienced by each of the spheres due to the presence of the other sphere, if each sphere is moving toward the origin at a speed $U_{o1}$ described by Eq. (8*a*). This force, $f(U_{o1},C_o/R_o)$, is a measure of the tendency of a neighboring inclusion to alter the densification behavior around a given test sphere. One can also learn from this quantity about the range of the interactions between the inclusions, i.e., how close they should be before appreciable interaction occurs. These are discussed further in the next section.

The second case which is of more interest is computation of the speed $\hat{W}_o$ for which $f(\hat{W}_o,C_o/R_o)$ would be equal to zero, and the corresponding stress fields in the matrix. For this purpose, we shall define a scaled approach velocity, $\omega$, as

$$\omega = \hat{W}_o/U_\infty \tag{27}$$

so that $\omega \to 1$ as $C_o/R_o \to \infty$. Here $U_\infty = -u_\infty(C_o)$ is determined from Eq. (7).

## IV. Results of the Two-Inclusions Problem

As one would intuitively expect, it was found that $f(U_{o1},C_o/R_o)$ is negative at all separations. At separations $C_o/R_o > \sim 3$, $|f|$ is negligibly small. As the separation is decreased, the attractive force increases rapidly at first and then levels off at close separations. At any given separation, as $\nu_m$ increases the attractive force is diminished.

Figure 2 describes the variation of the actual scaled approach velocity ($\omega$), dimensionless approach velocity in the absence of interactions ($U_{o1}/U_\infty$), and dimensionless approach velocity in the limit of only far-field interaction ($U_{o2}/2U_\infty$). As one would expect

$$U_{o1}/U_\infty < \omega < U_{o2}/2U_\infty$$

A significant departure of $\omega$ from $U_{o2}/2U_\infty$ implies appreciable near-field correction. Under these conditions, the matrix in the region between the particles experiences enhanced compression and this will lead to an increase in the densification rate in this region, as illustrated below.

The scaling for stress tensor defined by Eq. (13) is useful for the purpose of mathematical analysis. However, it is perhaps more convenient to plot the quantity $\sigma/\Sigma$ rather than $\sigma^*$ to get a better physical picture of the stresses experienced by the inclusions. Figure 3 presents the normal stress in the radial direction, hoop stresses, and the shear stress experienced by the inclusion particle for $\nu_m$ equal to 0.25 at a separation of $0.2R_o$. (When an external pressure $p_\infty$ is applied, the stresses in the matrix will be altered. However, as $\sigma^*$ is independent of $p_\infty$, the actual stresses on the surface of the inclusions can be easily deduced from Fig. 3 for any value of $p_\infty$.) The corresponding scaled densification rates in the matrix in the immediate vicinity of the surface of this inclusion are presented in Fig. 4. (This figure is valid for any $p_\infty$ as $\dot{\varepsilon}_\infty$ accounts for the effect of $p_\infty$ through Eq. (17).)

When the two inclusions are far apart, the densification rate is essentially uniform everywhere in the matrix. In contrast, when the inclusions are close to one another, a significant enhancement in the densification rate develops in the region between the inclusions, i.e., $\theta \sim 0°$. The enhancement becomes more and more pronounced as the separation between the particles decreases. In the two-inclusions problems, $\dot{\varepsilon}_\infty$ is the linear densification rate of the unreinforced matrix. It would be wrong to deduce from Fig. 4 that, except in a small region around $\theta \sim 55°$, the rate of densification of a matrix with inclusions is greater than that in an unreinforced matrix. A cumulative effect of all pairs of inclusions must be evaluated (see next section) before the model is compared with experimental data for a matrix containing many inclusions. When such a summation is carried out, it will be seen that a composite will densify at a slower rate than an unrein-

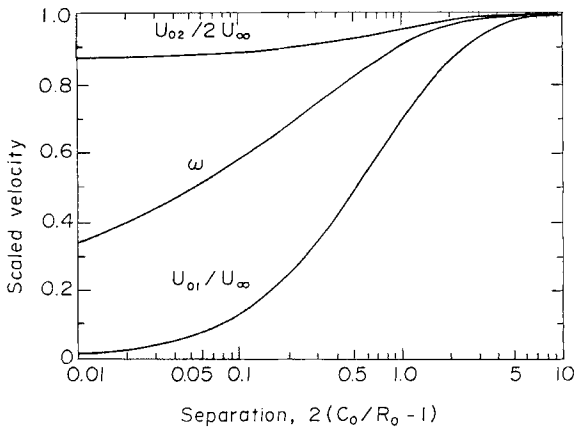


**Fig. 2.** Variation of scaled approach velocity as a function of separation.

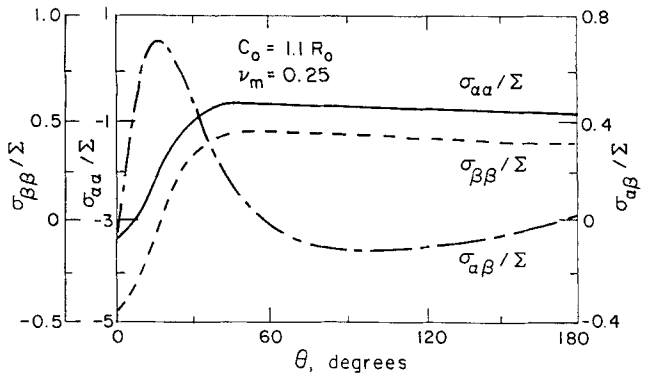


**Fig. 3.** Angular variation of the scaled stresses. See Fig. 1 for an explanation of how $\theta$ is measured. $\sigma_{\gamma\gamma} \equiv \sigma_{\beta\beta}$.

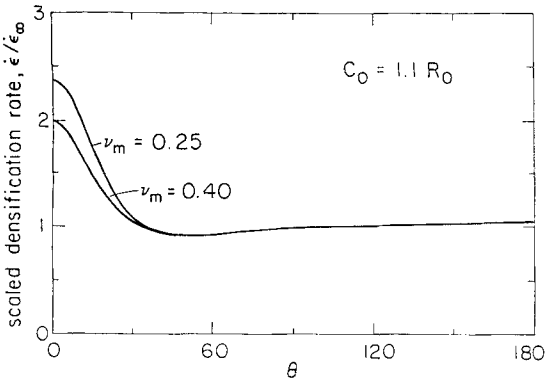


**Fig. 4.** Angular variation of the scaled densification rate.

forced matrix. Nevertheless, Fig. 4 suggests that in a matrix containing many inclusions, the rapid formation of an inflexible neck in the region between inclusions that are close together is quite possible, leading to the evolution of a rather rigid skeleton of inclusion particles (at sufficiently large volume fractions of the inclusions) as suggested by Lange.[10] We shall return to this point later in Section VI.

Scherer[1] and Bordia and Scherer[11] have argued that the radial stress acting on an inclusion particle in the case of pressureless sintering cannot exceed $2\Sigma$ in magnitude. We simply point out that such an assertion is dependent on the model used to analyze the problem. According to the composite sphere model analyzed by them, the maximum magnitude of the radial stress is equal to $2\Sigma(1 - 2\nu_m)/(1 + \nu_m)$. This maximum is equal to $0.8\Sigma$ and $2\Sigma$ for $\nu_m = 0.25$ and 0.0, respectively, which translates to values of 0.8 and 2.0 for $\sigma_{\alpha\alpha}/\Sigma$ in our analysis. A value of 0.8 for $\sigma_{\alpha\alpha}/\Sigma$ is indeed what we obtain in the case of $\nu_m = 0.25$ if the separation between the two inclusions is large. But at small separations, substantially larger values of $\sigma_{\alpha\alpha}/\Sigma$ can result in the gap between the particles, as seen in Fig. 3. Note that $\sigma_{\alpha\alpha}/\Sigma$ exceeds 2 in the gap even for $\nu_m = 0.25$. If we consider smaller values of $\nu_m$, this maximum will be even more pronounced. One can also show that the tensile hoop stresses in excess of $\Sigma(1 - 2\nu_m)/(1 + \nu_m)$ (which is the upper bound from composite sphere analysis[1]) can arise when the inclusions are close together. It must be added that the above discussion concerning the bounds is probably academic and that we do not present it as a basis for disputing the argument of Scherer[1] and Bordia and Scherer[11] that these sintering stresses are too weak to introduce flaws.

## V. Pairwise-Additive Treatment of the Multisphere Problem

It is well-known that the densification rate of a matrix containing rigid inclusions (henceforth composite) will decrease as the volume fraction of the inclusions increases. Experiments suggest that if the size of the inclusion particles is much larger than the characteristic size of the matrix particles, the only parameter through which the role of the inclusions enters into the densification rate of the composite is the volume fraction of the inclusions.[15] The simplest model to account for the role of inclusions on the linear densification rate of the composite, $\dot{\varepsilon}_c$, is the so-called rule of mixtures. Accordingly

$$(\dot{\varepsilon}_c)_{rm} = (1 - \nu_i)\dot{\varepsilon}_\infty \tag{28}$$

where $\nu_i$ is the volume fraction of the inclusions and $\dot{\varepsilon}_\infty$ is given by Eq. (17). But such a description overestimates the densification rate of the composite. This is due to the fact that the rule of mixtures does not account for the tensile stresses induced in the matrix by the inclusions (e.g., see Refs. 1, 11). More elaborate models such as the composite-sphere (CS) and self-consistent (SC) approximation have been described by Scherer[1] to account for the role of the inclusions. Accordingly

$$(\dot{\varepsilon}_c)_{CS} = \dot{\varepsilon}_\infty \left( \frac{1 - \nu_i}{1 + 2\dfrac{1 - 2\nu_m}{1 + \nu_m}\nu_i} \right) \tag{29}$$

$$(\dot{\varepsilon}_c)_{SC} = \dot{\varepsilon}_\infty \left\{ \frac{1 - \nu_i}{1 + \dfrac{2(1 - 2\nu_m)}{1 + \nu_m}\left[1 + \dfrac{15\nu_i(1 - \nu_m)}{2(1 - \nu_i)(4 - 5\nu_m)}\right]\nu_i} \right\} \tag{30}$$

If one assumes that the interactions between the inclusion particles are pairwise-additive, the rate of densification of the composite containing many spherical inclusions of uniform size can be deduced from the results described in the previous section as outlined below. Consider any inclusion as a reference and a spherical coordinate system whose origin coincides with that of this particle. Consider another test particle whose center is located at **r** in this coordinate system. This test particle will affect the stresses experienced by the reference particle as described in the earlier sections. Now, if the inclusions are distributed randomly in a matrix, it is reasonable to expect the distribution of the test particles around the reference particle to be spherically symmetric. Thus it makes sense to talk about the average normal stress imposed on the reference particle by test particles located at a distance $r$ and all possible orientations. In scaled form, this average normal stress arising from test particles located at a distance $r$ from the reference particle, $\hat{\sigma}^*_{RR}(r)$, is given by

$$\hat{\sigma}^*_{RR}(r) = \frac{1}{A}\int_A \sigma^*_{RR}\, dA \tag{31}$$

where $\sigma^*_{RR}$ in the right-hand side is evaluated on the surface of the reference particle and the integration is performed over the surface of the reference particle. One can show that

$$\hat{\sigma}^*_{RR}(r) \to \frac{3(1 - \nu_m)}{1 + \nu_m} \quad (\text{as } r \to \infty) \tag{32}$$

which is the single-sphere asymptote (deduced from Eq. (6)). As $r$ decreases, this stress steadily increases. Figure 5 describes the variation of $\hat{\sigma}^*_{RR}(1 + \nu_m)/3(1 - \nu_m)$ as a function of $r/R_o$ for three different values of $\nu_m$. As is evident in this figure, the radial dependence of $\hat{\sigma}^*_{RR}$ appears to be only small.

Now, to get the mean normal stress in the radial direction experienced by the reference particle, $\langle\sigma^*_{RR}\rangle$, we must average $\hat{\sigma}^*_{RR}$ over all possible values of $r$. Given the apparently small radial dependence of $\hat{\sigma}^*_{RR}$ one may, as a first approximation, say that

$$\langle\hat{\sigma}^*_{RR}\rangle \approx \frac{3(1 - \nu_m)}{1 + \nu_m} \equiv \langle\sigma^*_{RR}\rangle_o \tag{33}$$

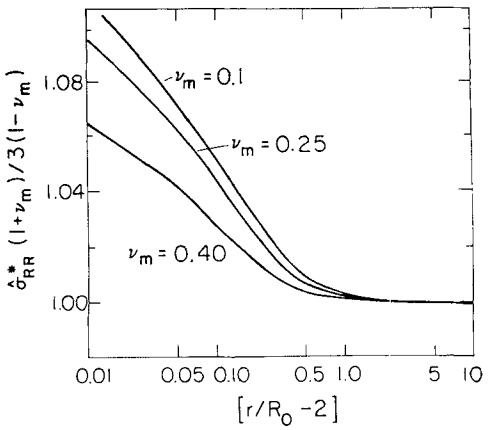


**Fig. 5.** Variation of $\hat{\sigma}^*_{RR}(1 + \nu_m)/3(1 - \nu_m)$ as a function of the dimensionless center-to-center distance $r/R_o$.

Such an idea has been previously described by Hsueh *et al.*[2]

Our entire analysis thus far has been concerned with the stress fields in the matrix. It is straightforward to compute the stresses in the interior of the reference particle, which is subjected to a mean normal stress in the radial direction (in scaled form) of $\langle\sigma^*_{RR}\rangle$. One then finds that inside the reference particle the radial and hoop stresses are equal, and in scaled form this stress is given by

$$\langle\sigma_i^*\rangle = \langle\sigma^*_{RR}\rangle \tag{34}$$

The quantity $\langle\sigma_i^*\rangle$ plays a key role in determining the densification rate of the composite material. The overall force balance equilibrium[2] dictates that

$$\nu_i\langle\sigma_i^*\rangle + (1 - \nu_i)\langle\sigma_m^*\rangle = 1 \tag{35}$$

where $\langle\sigma_m^*\rangle$ denotes the mean hydrostatic stress (in scaled form) in the matrix. (The right-hand side of Eq. (35) is unity, while a similar expression given by Hsueh *et al.*[2] has a value of zero. Both are equivalent and the apparent difference is simply due to the choice of scaling used in our study.) Furthermore, one can also show that the mean rate of (linear) densification of the matrix is simply equal to $\langle\sigma_m^*\rangle\dot{\varepsilon}_\infty$, where $\dot{\varepsilon}_\infty$ is described by Eq. (17). It then follows that

$$\dot{\varepsilon} \equiv (1 - \nu_i)\langle\sigma_m^*\rangle\dot{\varepsilon}_\infty = \dot{\varepsilon}_\infty(1 - \nu_i\langle\sigma_i^*\rangle) \tag{36}$$

If we consider the first approximation described by Eq. (33), the densification rate of the composite at this level of approximation, $\dot{\varepsilon}_{c1}$, is given by

$$\dot{\varepsilon}_{c1} = \dot{\varepsilon}_\infty\left[1 - \frac{3\nu_i(1 - \nu_m)}{1 + \nu_m}\right] \tag{37}$$

It is straightforward to show by a Taylor series expansion that one obtains the same result from Eqs. (29) and (30) as well. Thus, the first-order term in the densification models represents the cumulative effect of isolated inclusion-matrix interactions. The second-order term in a pairwise additive approximation represents the contribution arising from pair interactions. In the pairwise-additive treatment

$$\langle\sigma^*_{RR}\rangle = \langle\sigma^*_{RR}\rangle_o + \int_{r>2R_o} 4\pi\left[\hat{\sigma}^*_{RR} - \frac{3(1 - \nu_m)}{1 + \nu_m}\right]ng(r)r^2\,dr \tag{38}$$

where $n$ is the number density of the inclusions and $g(r)$ is the radial distribution function. For a random distribution of the inclusions, we may assume that $g(r) = 1$ for $r > 2R_o$. The matrix for each two-sphere problem in the above pairwise addition (Eq. (38)) is still the sintering matrix. A limitation of pairwise-additive treatment is readily apparent. The hydrodynamic interactions between the particles are necessarily many-body in nature, but are treated as only at pair level. For example, the effect of a particle far away from the reference particle will be severely modified by the presence of other particles in between, but the pairwise-additive treatment does not account for such shielding effects. A suggestion can be made to consider only the effects of immediate neighbors, as the interaction drops off rapidly as the separation between pairs of particles increases. But such an arbitrary truncation would be formally incorrect, as the hydrodynamic interaction does not decay rapidly enough, and as a result the integral in Eq. (38) is nonconvergent. To render it convergent, renormalization corrections have to be introduced, as discussed in detail by Chen and Acrivos.[19] The details of their mathematical treatment are not needed for our discussion. (Such a renormalization introduces an effective medium character to the matrix far away from the pair of spheres under consideration.) The rate of densification of the composite according to the pairwise-additive approximation deduced from Chen and Acrivos[19] analysis (cast in a rational form for ease of comparison with the CS and SC models) is given by

$$(\dot{\varepsilon}_c)_{pa} = \dot{\varepsilon}_\infty\left[\frac{1 - \nu_i}{1 + \dfrac{2(1 - 2\nu_m)}{1 + \nu_m}\nu_i + A_{pa}\nu_i^2}\right] \tag{39}$$

where the variation of $A_{pa}$ with $\nu_m$ is presented in Fig. 6. For the CS model, $A_{CS} = 0$. For the SC scheme, it follows from Eq. (30) that

$$A_{SC} = \frac{15(1 - 2\nu_m)(1 - \nu_m)}{(1 + \nu_m)(4 - 5\nu_m)} \tag{40}$$

which is also plotted in Fig. 6. These models differ at the level of pair approximation.

Experimental studies[14] have shown quite clearly the limitations in using the above models to describe the evolution of composite density as a function of time. When the volume fraction of spherical inclusions in an amorphous matrix exceeded roughly 0.12, the models grossly overestimated the rates of densification.[14] For such low critical volume fractions, the order $\nu_i^2$ terms in the pairwise-additive and SC schemes

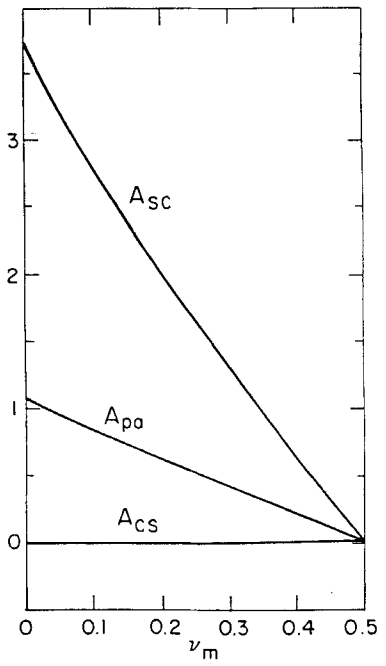


**Fig. 6.** Variation of $A_{pa}$, $A_{CS}$, and $A_{SC}$ with $\nu_m$.

are less than 3% of the order $v_i$ term. Considering that these densification models are quite idealized, it is dubious to take such a small correction too seriously. Thus the simpler version retaining only the first-order correction (namely, Eq. (29) or (37)) should suffice in this region. The order $v_i^2$ terms in the models are smaller (for $v_i < \sim 0.15$) than the scatter in the experimental data[14] on densification rates. A comparison of the available experimental data on amorphous matrices with the SC scheme has already been published.[14] Noting that the pairwise-additive treatment does not yield predictions which depart significantly from the CS and SC schemes (for $v_i < \sim 0.12$), it does not serve any useful purpose to present a comparison of the pairwise-additive treatment with the available experimental data. While it is true that all three models overestimate the experimental data on densification rates[14] when $v_i > \sim 0.12$, the models themselves differ very little from each other even for much larger volume fractions. Thus the failure of these models stems from one or more important physical considerations not accounted for in all these models.

The formation of percolation clusters (of inclusion) that control the deformation of the composite (when $v_i > \sim 0.16$, the percolation threshold for uniform spheres) and which is not accounted for in any of the models has been suggested[1,11] as the reason for the failure of the models. Having a $v_i > \sim 0.16$ alone is not a sufficient condition for the formation of percolation clusters that are not easily deformed. A necessary condition is the existence of a barrier hindering the independent movement of nearby particles (e.g., compare with flocculated and dispersed colloidal suspensions). In the case of an amorphous matrix that wets the inclusions (and assuming that other direct interactions do not exist between the inclusions), one is then faced with the question as to how such a barrier arises. The analysis presented in this paper shows that when inclusions are close together, densification occurs at a faster rate in the gap between these particles than elsewhere and this serves to bridge the particles together producing a barrier for the independent movement of these particles. Thus, we suggest that the occurrence of *nonuniform densification* leading to the formation of an inflexible skeleton when the percolation threshold is exceeded is an important feature that controls the deformability of the composite.

The importance of nonuniform densification in the failure of the models may be easily tested experimentally as follows. If the amorphous matrix is uniformly distributed in the beginning, then at time zero, even if $v_i$ is greater than the percolation threshold, the deformation of the composite should not be controlled by the percolation clusters, provided our argument that a bridge must first be formed between the percolation network of particles is correct. This implies that if the above densification models are used to predict only the *initial* rate of densification, then these models should succeed for $v_i$ well in excess of a percolation threshold. It would be useful to test this experimentally so that one can pinpoint the reason for the failure of the sintering models.

It should be pointed out that the nonuniformity in the densification of the composite is not quantitatively captured by the two-inclusions analysis discussed in the previous sections. A more accurate analysis should examine the interaction between these two spheres in the presence of all other spheres in the composite. Treating such a multisphere problem is beyond the scope of this study. However, it is interesting to consider the excluded-volume effect of the other spheres on the interactions between two spheres, as described in the next section.

It is also important to point out that the above discussion is limited to the case of amorphous matrices. It is known that in the context of polycrystalline matrices, the presence of inclusions at much lower levels ($v_i < \sim 0.05$) where the interaction between inclusions is unimportant is often enough to cause a drastic reduction in the sintering rate of the composite, and the models discussed here are hardly applicable.

## VI. Excluded-Volume Effect

Consider an isotropic amorphous matrix containing rigid spherical inclusions distributed randomly at a number density $n$. Also consider a reference inclusion particle and a spherical coordinate system whose origin coincides with the center of this sphere. Clearly there will be no particle whose center lies within the sphere of radius $2R_o$ from the origin. Consider a point at a distance $2C_o$ away from the origin ($2C_o > 2R_o$) where we are planning to place the center of a second particle in a thought experiment. By placing this particle, we are excluding particle centers from a sphere of radius $2R_o$ around this particle. (When $2C_o < 4R_o$, the additional volume excluded by the second sphere will be somewhat smaller because of the overlap of the excluded volumes of the references and second particles.) To a first approximation, one can say that the force experienced by the reference particle in the direction of this second particle is equal to the force experienced by the reference sphere due to the second sphere minus the force on the reference sphere arising from a statistical distribution of sphere centers on the volume excluded by the second sphere. These forces will still be computed in our analysis in a pairwise-additive manner.

The effective force between the reference particle and the second particle, $\mathbf{F}_{eff}$, which will be acting along the line of centers is thus given by

$$\mathbf{F}_{eff} = \mathbf{F}_1 - \mathbf{F}_2 \tag{41}$$

where $\mathbf{F}_1$ is the force due to the second sphere alone and is given by analysis in Section III (for example, see Eq. (25)) and $\mathbf{F}_2$ is the contribution due to the particles that were excluded by the second sphere. Expressing in scaled form, as in Section III, by dividing by $-R_o^2\Sigma(1 + p_\infty/\Sigma)$

$$f_{eff} = f_1 - f_2 \tag{42}$$

where a negative $f_{eff}$ implies an effective attractive interaction between the two spheres. The variation of $f_1$ with separation has been discussed in Sections III and IV. It is quite straightforward to show that

$$f_2 = \int_{r_{min}}^{r_{max}} \pi r^2 n f_1(r)\, g(r) \left[1 - \left(\frac{r^2 + 4C_o^2 - 4R_o^2}{4C_o r}\right)^2\right] dr \tag{43}$$

where $r_{max} = 2(C_o + R_o)$ and $r_{min} = 2(C_o - R_o)$ or $2R_o$, whichever is larger. For a random distribution, $g(r) = 1$ for $r > 2R_o$. One can then write Eq. (42) as

$$f_{eff}(C_o/R_o) = f_1(C_o/R_o)[1 - v_i h(C_o/R_o)] \tag{44}$$

where $h(C_o/R_o)$ can be deduced from Eq. (43). The variation of $h$ as a function of the separation between the reference particle and the second particle is shown in Fig. 7. Computa-

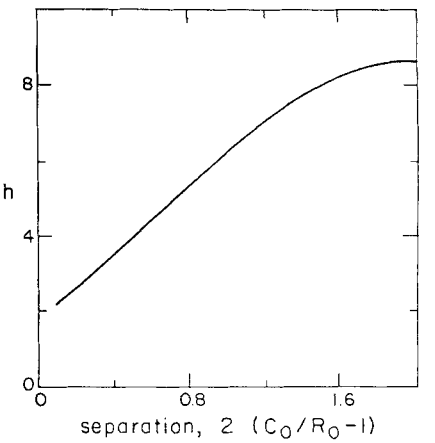


**Fig. 7.** Variation of $h$ with separation between the particles.

tions revealed that the function $h$ is essentially independent of $\nu_m$. Within the framework of the excluded-volume analysis, the function $h$ is independent of $v_i$ as well. Thus for a given separation between the reference particle and the second particle, the interaction is attractive if $v_i$ is less than $1/h$, and repulsive otherwise. Stated in a somewhat different but equivalent way, for any given $v_i$, there is a critical separation above which the interaction between the particles is repulsive, while for particle separations below this critical value the force is attractive, as pointed out heuristically by Lange.[10]

It is interesting to examine more closely this critical separation. For each given $v_i$, let us define an average spacing between particle centers assuming a simple cubic packing, i.e.

$$\langle C_o/R_o \rangle = (\pi/6v_i)^{1/3} \tag{45}$$

From Eq. (44) and Fig. 7, one can also determine the critical value of $C_o/R_o$ for which the net interparticle force will be equal to zero. Let us denote this critical separation by $(C_o/R_o)_c$. Figure 8 shows a plot of $(C_o/R_o)_c$ vs $\langle C_o/R_o \rangle$. In the range of center-to-center separations shown in this figure, the critical separation is essentially equal to the average separation between the particles. (This discussion is limited to only spherical particles.) Thus, in the course of viscous densification of a composite, faster-than-average densification of the matrix can be expected on the gaps between particles whose separation is below the average value. The overall densification rate of the composite is still given by Eq. (39).

## VII. Summary

The interaction between two rigid spherical inclusions in an infinite viscously densifying matrix has been analyzed. Following Scherer,[1] the relationship between stress and strain rate in the matrix has been assumed to be linearly viscous. The two spheres are shown to interact attractively, which in turn induces an enhanced densification in the region between the two spheres. This enhancement becomes more pronounced as the gap between the two spheres is decreased. Highly nonuniform stress fields are shown to arise in the vicinity of the two spheres.

An expression is obtained for the rate of densification of the composite (matrix + inclusions) by statistically averaging over all possible configurations of the two-sphere geometry.

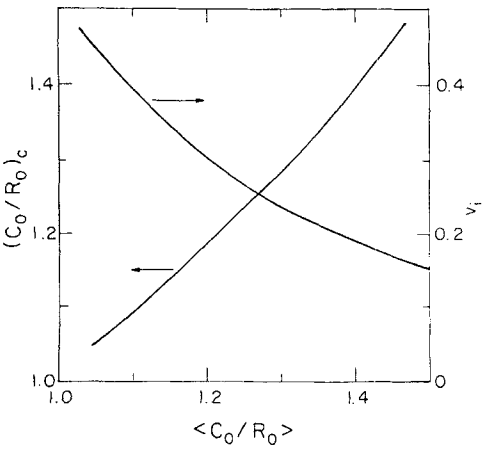


**Fig. 8.** Dependence of $(C_o/R_o)_c$ on $\langle C_o/R_o \rangle$. Also shown are the variations of the volume fraction of inclusions with $\langle C_o/R_o \rangle$ as given by Eq. (45).

This result is compared with the CS and SC models that have been discussed in the literature.[1] All these models are identical to order $v_i$ (where $v_i$ is the volume fraction of the inclusions), which represents the cumulative effect of isolated inclusion-matrix interactions. These models differ from one another in the order $v_i^2$ term, which represents the contributions from interactions between pairs of inclusions. All these models are known to grossly overestimate the densification rates of composite materials when the volume fraction of the inclusions approaches the percolation threshold. However, the models themselves differ very little from each other even for a much larger volume fraction of inclusions.

Although the interaction between two spheres in an infinite matrix is always attractive, the presence of other inclusions in the matrix can alter the nature of the interaction between these two particles. This modification comes about because of the excluded-volume effect and also many-body effects. Focusing on the excluded-volume effect, it is shown that for composite materials, there is a critical separation above which the interactions between the particles are repulsive, while for particle separations below this critical value the interactions are attractive.[10] This critical separation is a function of the volume fraction of inclusions and is essentially equal to the average separation between the inclusions.

**Acknowledgments:** We are delighted to acknowledge the many helpful criticisms provided by the reviewers.

## References

[1]G.W. Scherer, "Sintering with Rigid Inclusions," *J. Am. Ceram. Soc.*, **70** [10] 719–25 (1987).
[2]C. H. Hsueh, A. G. Evans, and R. M. McMeeking, "Influence of Multiple Heterogeneities on Sintering Rates," *J. Am. Ceram. Soc.*, **69** [4] C-64–C-66 (1986).
[3]A. G. Evans, "Considerations of Inhomogeneity Effects in Sintering," *J. Am. Ceram. Soc.*, **65** [10] 497–501 (1982).
[4]R. Raj and R. K. Bordia, "Sintering Behavior of Bimodal Compacts," *Acta Metall.*, **32** [7] 1003–19 (1984).
[5]C. H. Hsueh, A. G. Evans, R. M. Cannon, and R. J. Brook, "Viscoelastic Stresses and Sintering Damage in Heterogeneous Powder Compacts," *Acta Metall.*, **34** [5] 927–36 (1986).
[6]C. H. Hsueh, "Sintering Behavior of Powder Compacts with Multiheterogeneities," *J. Mater. Sci.*, **21**, 2067–72 (1986).
[7]L. C. De Jonghe, M. N. Rahaman, and C. H. Hsueh, "Transient Stresses in Bimodal Compacts During Sintering," *Acta Metall.*, **34** [7] 1467–71 (1981).
[8]K. D. Reeve, "Non-Uniform Shrinkage in Sintering," *Am. Ceram. Soc. Bull.*, **42** [8] 452 (1963).
[9]F. F. Lange and M. Metcalf, "Agglomerate Motion and Cracklike Internal Surface Caused by Differential Sintering," *J. Am. Ceram. Soc.*, **66** [6] 398–406 (1983).
[10]F. F. Lange, "Constrained Network Model for Predicting Densification Behavior of Composite Powders," *J. Mater. Res.*, **2** [1] 59–65 (1987).
[11]R. K. Bordia and G.W. Scherer, "Constrained Sintering: III. Rigid Inclusions"; to be published in *Acta Metall.*
[12]R. K. Bordia and R. Raj, "Sintering of $TiO_2(Al_2O_3)$ Composites: A Model Experimental Investigation," *J. Am. Ceram. Soc.*, **71** [4] 302–10 (1988).
[13]R. K. Bordia and R. Raj, "Hot Isostatic Pressing of Ceramic/Ceramic Composites at Pressure Below 10 MPa," *Adv. Ceram. Mater.*, **3** [2] 122–26 (1988).
[14]M. N. Rahaman and L. C. De Jonghe, "Effect of Rigid Inclusions on the Sintering of Glass Powder Compacts," *J. Am. Ceram. Soc.*, **70** [12] C-348–C-351 (1987).
[15]M.W. Weiser and L.C. De Jonghe, "Inclusion Size and Sintering of Composite Powders," *J. Am. Ceram. Soc.*, **71** [3] C-125 (1988).
[16]J. F. Shelley and Y.Y. Yu, "The Effect of Two Rigid Spherical Inclusions on the Stresses in an Infinite Elastic Solid," *J. Appl. Mech.*, **33**, 68–74 (1966).
[17]J. Happel and H. Brenner, Low Reynolds Number Hydrodynamics; pp. 516–19. Prentice-Hall, Englewood Cliffs, NJ, 1965.
[18]G.W. Scherer, "Sintering of Inhomogeneous Glasses: Application to Optical Waveguides," *J. Non-Cryst. Solids*, **34**, 239–56 (1979).
[19]H.-S. Chen and A. Acrivos, "The Effective Elastic Moduli of Composite Materials Containing Spherical Inclusions at Non-Dilute Concentrations," *Int. J. Solids Struct.*, **14**, 349–64 (1978). □